HHS Public Access

Author manuscript

Conf Proc IEEE Eng Med Biol Soc. Author manuscript; available in PMC 2016 March 14.

Published in final edited form as:

Conf Proc IEEE Eng Med Biol Soc. 2015 August ; 2015: 1993–1996. doi:10.1109/EMBC.2015.7318776.

Registration of Coronary Arteries in Computed Tomography Angiography Images using Hidden Markov Model

Yuxuan Luo[1], **Jianjiang Feng**[1], **Miao Xu**[1], **Jie Zhou**[1], **James K. Min**[2], and **Guanglei Xiong**[2]

Yuxuan Luo: luoyx12@mails.tsinghua.edu.cn; Jianjiang Feng: jfeng@tsinghua.edu.cn; Miao Xu: xum14@mails.tsinghua.edu.cn; Jie Zhou: jzhou@tsinghua.edu.cn; James K. Min: jkm2001@med.cornell.edu; Guanglei Xiong: gux2003@med.cornell.edu

[1]Department of Automation, Tsinghua University, Beijing, China

[2]Dalio Institute of Cardiovascular Imaging, Department of Radiology, Weill Cornell Medical College, NY 10021, USA

Abstract

Computed tomography angiography (CTA) allows for not only diagnosis of coronary artery disease (CAD) with high spatial resolution but also monitoring the remodeling of vessel walls in the progression of CAD. Alignment of coronary arteries in CTA images acquired at different times (with a 3–7 years interval) is required to visualize and analyze the geometric and structural changes quantitatively. Previous work in image registration primarily focused on large anatomical structures and leads to suboptimal results when applying to registration of coronary arteries. In this paper, we develop a novel method to directly align the straightened coronary arteries in the cylindrical coordinate system guided by the extracted centerlines. By using a Hidden Markov Model (HMM), image intensity information from CTA and geometric information of extracted coronary arteries are combined to align coronary arteries. After registration, the pathological features in two straightened coronary arteries can be directly visualized side by side by synchronizing the corresponding cross-sectional slices and circumferential rotation angles. By evaluating with manually labeled landmarks, the average distance error is 1.6 mm.

I. INTRODUCTION

Coronary artery disease (CAD) is one of the leading causes of death throughout the world [6]. Recently, computed tomography angiography (CTA) has emerged as a promising non-invasive option for coronary angiography, with significant advances in temporal resolution and volume coverage now allowing for acquisition of virtually motion-free images at isotropic spatial resolution at 500 μm. Compared to invasive reference standards, CTA has been demonstrated to have high diagnostic accuracy for anatomic stenosis detection [5]. However, the large amount of data in a 3D CTA image also poses considerable challenges for accurate quantification and staging of CAD manifestation. Furthermore, diagnosis using multiple image volumes acquired of the same patient at different times (e.g. initial visit vs. follow-ups) is often needed in clinical practice to monitor the progression of CAD.

Like other human organs, coronary arteries constantly adapts to hemodynamic, metabolic, and inflammatory stimuli by geometric and structural remodeling of the vessel wall during the development of atherosclerosis. Although CTA allows for visualizing vessel walls with exquisite spatial resolution, temporal resolution remains limited. Deformation of coronary arteries inevitably occurs even during the same scan due to cardiac and respiratory motion. In addition, significant rigid (e.g. change in coordinate system and scanning direction) and nonrigid transformation (difference in patient pose, heart rate, acquisition time within the cardiac cycle) are also present in CTA images. To enable direct comparison of coronary artery anatomy, alignment of two different images is a prerequisite to allow for detection of actual wall remodeling, especially for the patients with stenosis of intermediate grades. Deformable image registration is an active research topic in medical image analysis and has been applied to align anatomical structures with different levels of success. However, most previous work has been focused on registration of structures with volumetric shapes. Although they can be applied to register coronary arteries with tubular shapes, the performance is usually suboptimal because the results tend to favor better alignment of neighboring structures with larger volume, e.g. myocardium and lungs. In this paper, we develop a novel automated method to register coronary arteries directly by using Hidden Markov Model [7] applied in the straightened vessel segments.

II. Methods

According to [8], medical image registration algorithms are composed of three key components: deformation model, matching criterion and optimization method. In this section, we will introduce our method following this schema. Section II-A will introduce our curve based deformation model, Section II-B illustrates the matching criterion and Section II-C will introduce optimization method designed for our model. Finally, Section II-D will describe the semi-automatic method we use to extract centerlines for completion.

A. Deformation Model

Deformation models used in medical image registration include simple parametric transforms such as rigid, similar, homogeneous transforms and more complex geometric transformations based on interpolation such as Thin Plate Spline model [1] or Free Form Deformations coupled with B-spline [2]. All these models are designed for general registration of structures with volumetric shapes. In this paper, we focus on alignment of coronary artery and propose a more efficient domain-specific deformation model. Instead of computing correspondences directly in Cartesian coordinate system, we first extract coronary artery centerlines from CTA image and then infer relative offset and rotation between them in cylindrical coordinate system.

Given an artery centerline, straightened curved planar reformation (SCRP) [4] is a common method for displaying coronary artery clinically. It defines a mapping from 3D space to 2D image plane, each horizontal line of which corresponds to a diameter of the circle centered at a specific point on the centerline. The vertical offset on SCRP indicates the geographic distance from the starting point of centerline. To identically determine a SCRP, an angle-of-interest should be assigned to each point on the centerline because we have to select one

direction of the diameter on each cross-sectional slice. In practice, only the angle-of-interest of the starting point of the curve is sufficient to display a single tubular structure by using rotation-minimizing frames[9]. However, when comparing two different CTA images of the same patient, misalignment can be large before registration.

A curve used to generate SCRP can be represented as:

$$\{C(t)=X(t), Y(t), Z(t), \theta(t) | t \in [0, L]\},$$

where t is geographic distance between a specific point and the starting point; L is the length of the curve; $X(t)$, $Y(t)$, $Z(t)$ are the Euclidean coordinates and $\theta(t)$ represents the relative angle-of-interest (angle between a user-specific direction and the one inferred by using rotation-minimizing frames).

Given the fixed centerline C_f and moving centerline C_m, we define our deformation model as:

$$\{l(t_f), d\theta(t_f) | t_f \in [0, L]\}.$$

It pairs points from C_f and C_m by:

$$C_f(t_f) \rightleftarrows \{X_m(t_m), Y_m(t_m), Z_m(t_m), \theta(t_m)+d\theta(t_f)\},$$

$$\text{where } t_m=l(t_f).$$

This model is sufficient to describe the actual deformation given artery centerline while simplifying the search space dramatically. In fact, we transform sophisticated free 3D registration problem to a more tractable one in cylindrical coordinate system (see Fig. 2).

In order to optimize our parametrized model, we discretize the curves by evenly sampling points from C_f and C_m with predefined step δl and discrete θ with step $\delta\theta$. After that, deformation model can be described just by a series of discrete status on the fixed curve:

$$\{S_i=\{l_i, d\theta_i\} | i \in \{0, 1, \ldots, N_f\}\},$$

where i and N_f are the index and total number of sampled points on C_f respectively, l and $d\theta$ represent the discretized location and relative rotation of the corresponding point of *ith* control point on C_m. The curve between consecutive points with a small interval should be smooth, so we further sample the control points with a fixed interval K. Overall, our model can be concisely described by:

$$\mathscr{S} := \{S_{cp_i} | cp_i=i*K, i \in \{0, 1, \ldots, N_{cp}\}\}.$$

The status of inner points can be naturally interpolated linearly. Discretion and sub-sampling decreases the theoretical high bound of registration accuracy, but can achieve better result in practice because it avoids potential over-fitting and makes the global optimization more tractable.

B. Matching Criterion

In [8], the authors separated matching criterion and regulation term for clarity. In this work, we just treat them as two types of similarity - image similarity (matching criterion) and geometric similarity (regulation). Although status in our model are defined on each point, similarity is measured pair-wisely because segment correspondence determined by two consecutive status is much more robust than a single pair of cross-sectional slices.

Here, normalized correlation coefficient (NCC) is adopted to measure the similarity between images. For *ith* segment, we generate two cylinder $\boldsymbol{cyl}_i^m$ and $\boldsymbol{cyl}_i^f$ around moving and fixed centerline:

$$\boldsymbol{cyl}_i^m = \mathrm{Cylinder}(I_m, C_m, \theta_{l_{cp_i}} + d\theta_{cp_i}, l_{cp_i}, l_{cp_{i+1}})$$

$$\boldsymbol{cyl}_i^f = \mathrm{Cylinder}(I_f, C_f, \theta_{cp_i}, cp_i, cp_{i+1}),$$

where Cylinder(*I*, *C*, θ, *start*, *end*) extracts cylinder around centerline *C* from image *I*. θ, *start*, *end* indicate angle-of-interest, start point and end point of curve segment of interest respectively. Certain layers (10 in our experiment) of cross-sectional slice compose a cylinder and for each layer of a cylinder, we sample the voxels with step δ*R* radially and δθ circumferentially on cross-sectional slice within radius *R*. Finally, the image similarity of *ith* segment is:

$$\mathrm{P}_{img}^{(i)} := \mathrm{NCC}(\boldsymbol{cyl}_i^m, \boldsymbol{cyl}_i^f).$$

Deformation regulation is also imposed because the length of centerline should not vary too much and relative angle should change smoothly. We limit the change of the angle between two consecutive control points to Θ_{max} and the length to $[r_{min}, r_{max}]*K*\delta l$. Within that reasonable range, a pairwise similarity term P_{geo} is used to regulate the deformation:

$$\mathrm{P}_{geo}^{(i)} := 1 - |\log(\frac{l_{cp_{i+1}} - l_{cp_i}}{K})|.$$

In summary, the similarity between two arteries given $\mathscr{S}$ is represented by:

$$J(\mathscr{S}) := \sum_{i=1:N-1} w_{img} * \mathrm{P}_{img}^{(i)} + w_{geo} * \mathrm{P}_{geo}^{(i)}.$$

C. Optimization Method

To accelerate our algorithm, we adopt a coarse-to-fine strategy. First, we coarsely align two arteries with single offset and rotation. It aligns two centerlines coarsely with a rigid transform under cylinderical coordinate system.

In the second step, the alignment is refined by an optimization problem:

$$\mathscr{S}^* = \underset{S_{cp_i}, i=1:N}{\operatorname{argmax}} J(\mathscr{S}).$$

Notice J only relies on pairwise discrete status. Our problem is a specific case of Hidden Markov Model without an unary term and Viterbi algorithm can be used to infer the global maximum [7].

D. Centerline Extraction

Because our attention is on registration, we just implement an simple two-point method based on shortest path with Frangi vesselness [3]. Registration process we proposed does not account for relative offset on the normal plane, so it is sensitive to the inaccuracy of centerline extraction. To minimize the influence of limited accuracy of our simple extraction algorithm, centerlines are slightly manually refined with the help of a learning-based lumen segmentation method.

III. Experiments

In this work, our experiments were performed on five pairs of CTA images[1]. Each pair was acquired with an interval of 3–7 years. Left anterior descending artery (LAD), left circumflex artery (LCX), right coronary artery (RCA) were extracted from every CTA image and the algorithm proposed in this work was used to align them. Parameters are fixed in all cases, as listed in Table I (s_{img} represents the default value of P_{img} when corresponding point is out of the range).

Fig. 3 and Fig. 4 show the examples of SCRPs and cross-sectional slices before and after registration. After registration, two centerlines are better aligned. Fig. 5 shows two cases with stenosis and calcification in detail, where the automatic alignment result is close to manual alignment and visualization of pathological features is clear.

To quantitatively evaluate the accuracy of our algorithm, we manually label 7–24 corresponding landmarks of each pair of coronary arteries that can accurately align fixed and moving coronary artery centerlines with Thin Plane Spline [1]. Our algorithm is evaluated by comparing the average distance between the transformed points and the manually labeled ones. The average distance error is 1.6 mm. In Table II, E_{g+i} indicates the average distance error and standard deviation of each pair of artery using our algorithm and E_i indicates results when we relax geometric constraints ($w_{geo} = 0$, $r_{min,max} = [0.6, 1.4]$ and $\Theta_{max} = 30°$). It is clear that both image and geometry are important.

[1]The experimental procedures involving human subjects described in this paper were approved by the Institutional Review Board.

IV. CONCLUSIONS and Future Work

In this work, we propose an algorithm to align two arteries of the same patient acquired with an interval of 3–7 years. Experiments shows that our algorithm can achieve a good accuracy according to manual registration and pathological features can be directly visualized side by side.

Since our algorithm relies on the extraction of artery centerlines, the registration will fail if the extracted centerline is far away from the true centerline. Improvements to handle inaccurate centerlines will be our future work.

Acknowledgments

This work was supported by the National Natural Science Foundation of China under Grants 61225008, 61373074 and 61020106004, the National Basic Research Program of China under Grant 2014CB349304, the Ministry of Education of China under Grant 20120002110033, the Tsinghua University Initiative Scientific Research Program, and NIH R01HL115150.

References

1. Bookstein FL. Principal warps: Thin-plate splines and the decomposition of deformations. IEEE Transactions on Pattern Analysis and Machine Intelligence. 1989; 11(6):567–585.
2. Declerck J, Feldmar J, Goris ML, Betting F. Automatic registration and alignment on a template of cardiac stress and rest reoriented spect images. IEEE Transactions on Medical Imaging. 1997; 16(6):727–737. [PubMed: 9533574]
3. Frangi, AF.; Niessen, WJ.; Vincken, KL.; Viergever, MA. Proc. Medical Image Computing and Computer-Assisted Interventation (MICCAI). Springer; 1998. Multiscale vessel enhancement filtering; p. 130-137.
4. Kanitsar A, Fleischmann D, Wegenkittl R, Felkel P, Groller ME. Cpr-curved planar reformation. Proc. IEEE Visualization. 2002:37–44.
5. Min JK, Shaw LJ, Berman DS. The present state of coronary computed tomography angiography: a process in evolution. Journal of the American College of Cardiology. 2010; 55(10):957–965. [PubMed: 20202511]
6. Murray CJ, Lopez AD. Alternative projections of mortality and disability by cause 1990–2020: Global burden of disease study. The Lancet. 1997; 349(9064):1498–1504.
7. Rabiner L, Juang B-H. An introduction to hidden markov models. ASSP Magazine, IEEE. 1986; 3(1):4–16.
8. Sotiras A, Davatzikos C, Paragios N. Deformable medical image registration: A survey. IEEE Transactions on Medical Imaging. 2013; 32(7):1153–1190. [PubMed: 23739795]
9. Wang W, Joe B. Robust computation of the rotation minimizing frame for sweep surface modeling. Computer-Aided Design. 1997; 29(5):379–391.

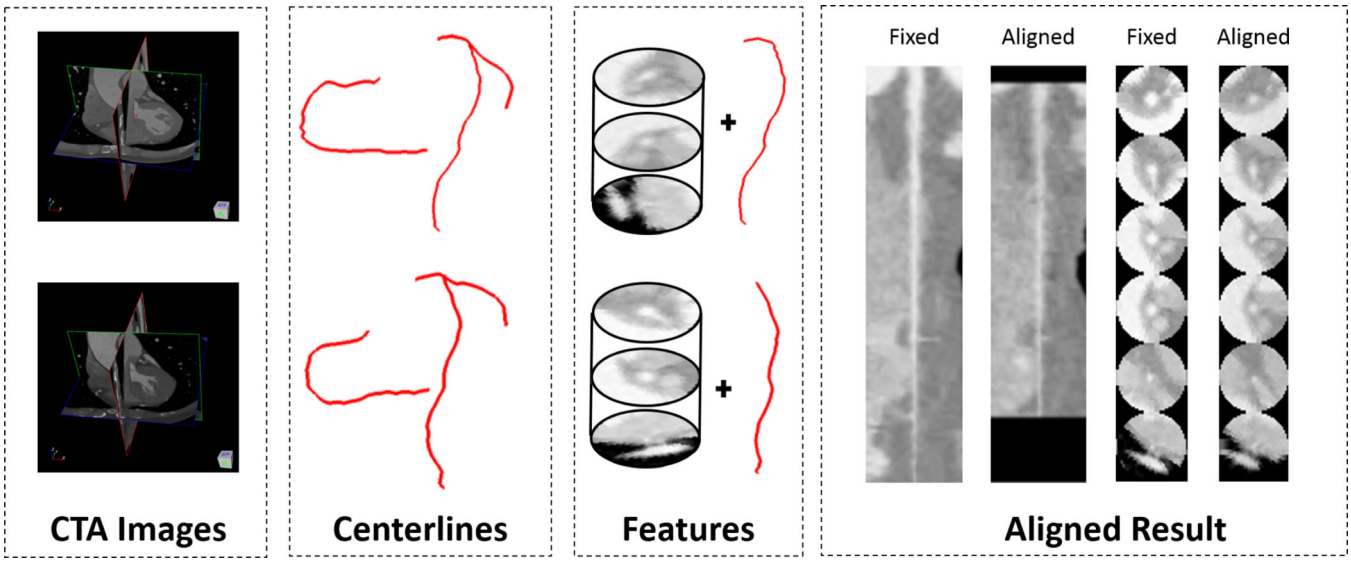

Fig. 1.

Flowchart of our method. We first extract centerlines from two CTA images acquired at different times and utilize the image information around centerline to align them.

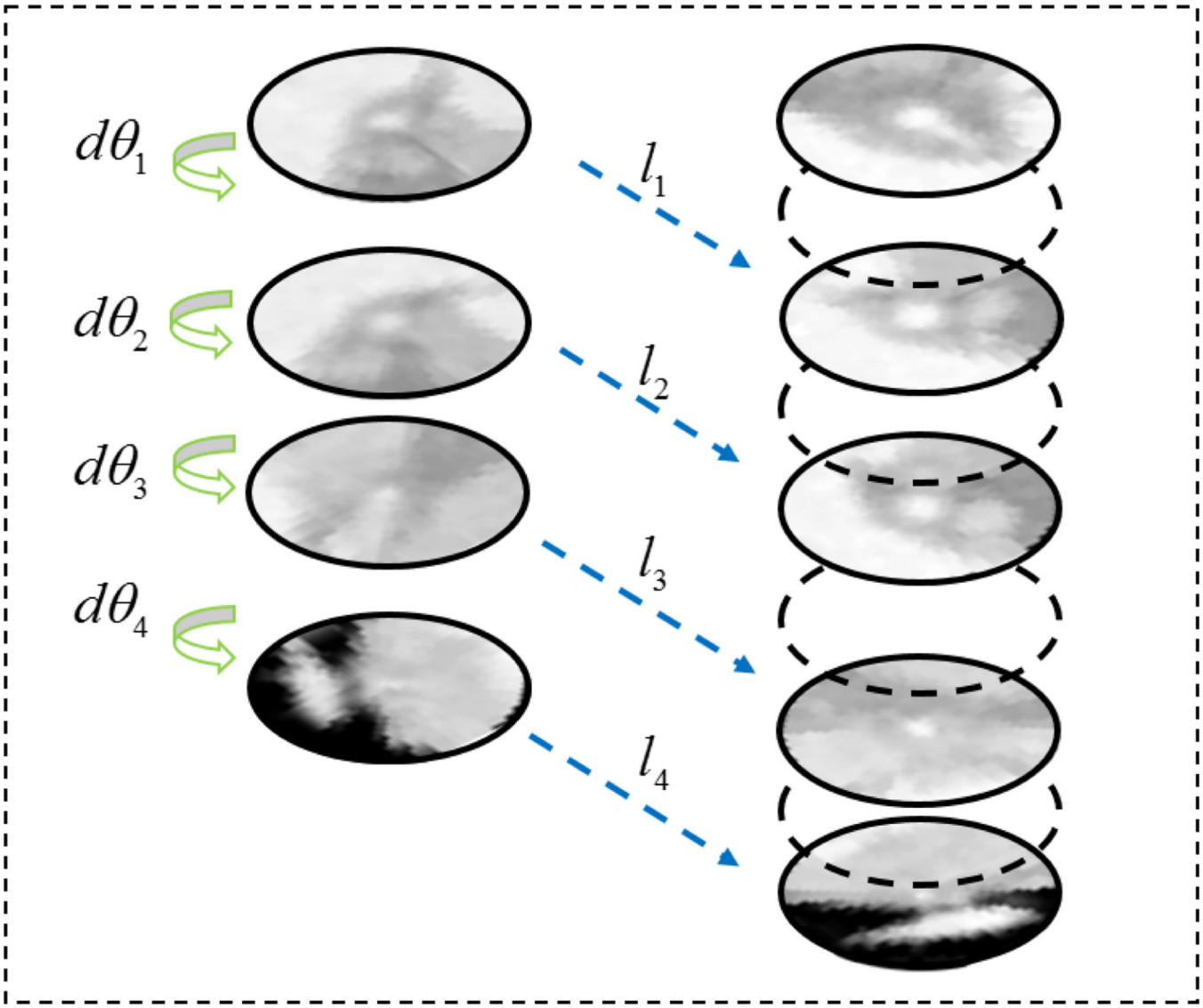

Fig. 2.

An illustration of our deformation model. To align two arteries, two variables are assigned to each point (represented by its cross-sectional slice) from a fixed centerline(left) - $d\theta$ determines the relative rotation and l counts for offset along the centerline. Dash circles on the right column indicate the interpolated points between control points.

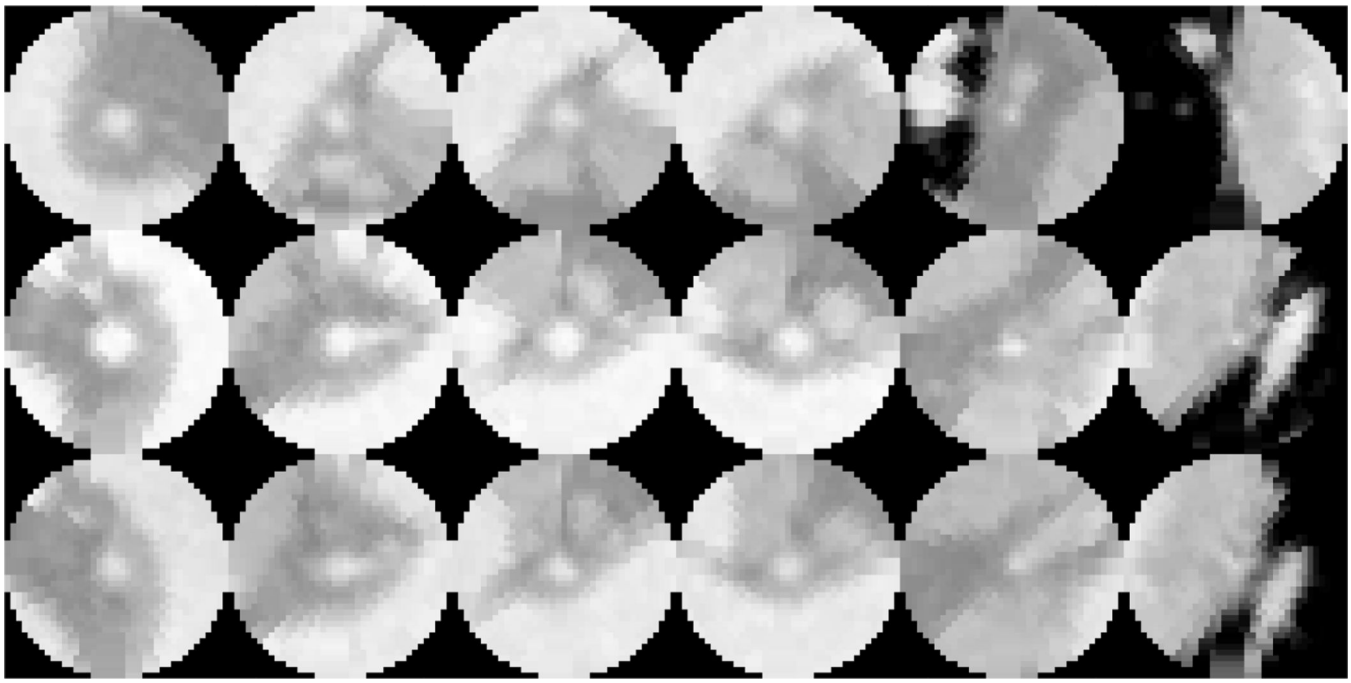

Fig. 3.

An example of our registration result. The three rows are some cross-sectional slices that are sampled around moving centerline, fixed centerline and aligned centerline, respectively. The columns show different locations along the centerline.

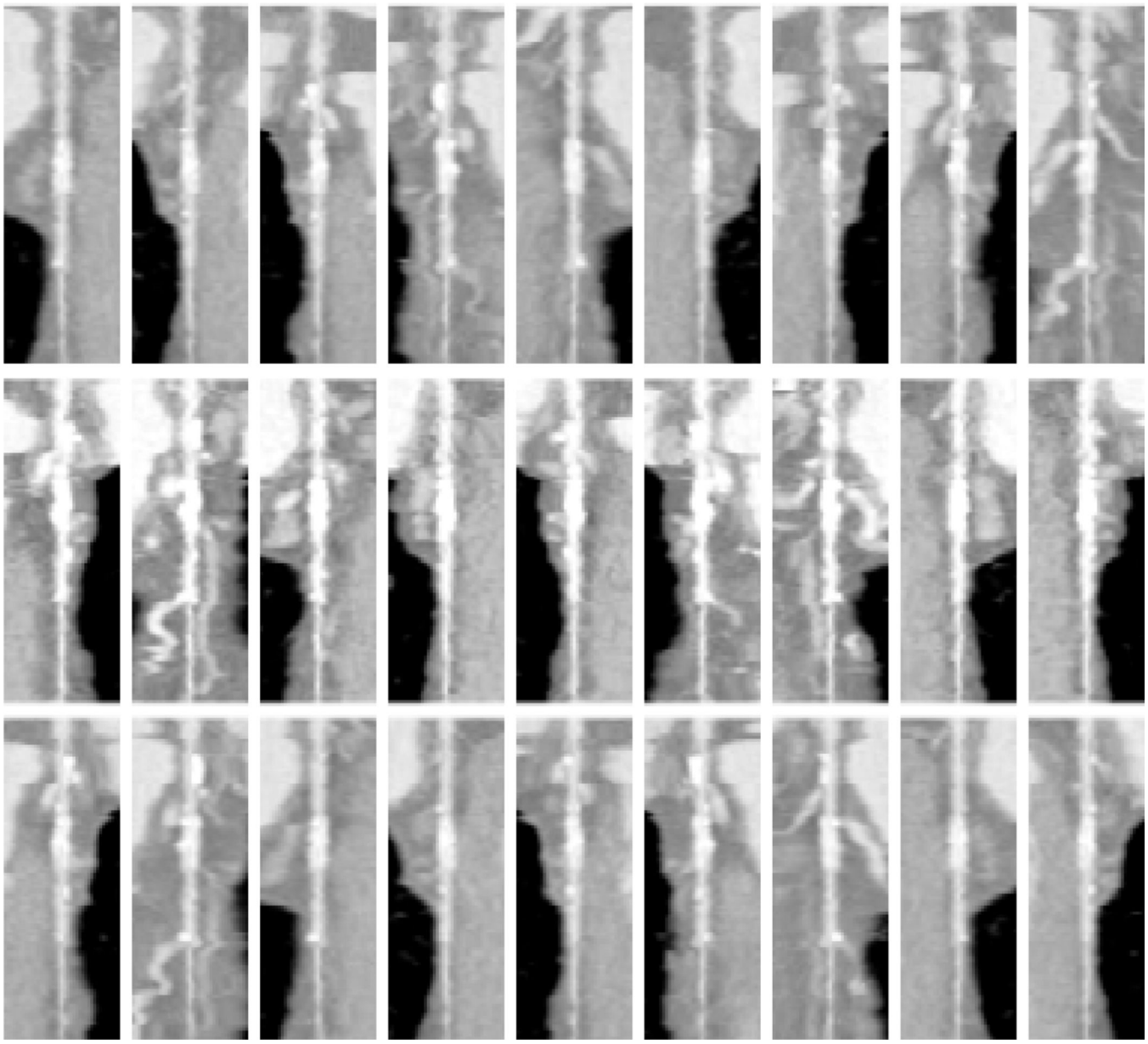

Fig. 4.

An example of our registration result. The three rows of SCRP are generated from moving centerline, fixed centerline and aligned centerline respectively. The columns represent different corresponding angles of interest.

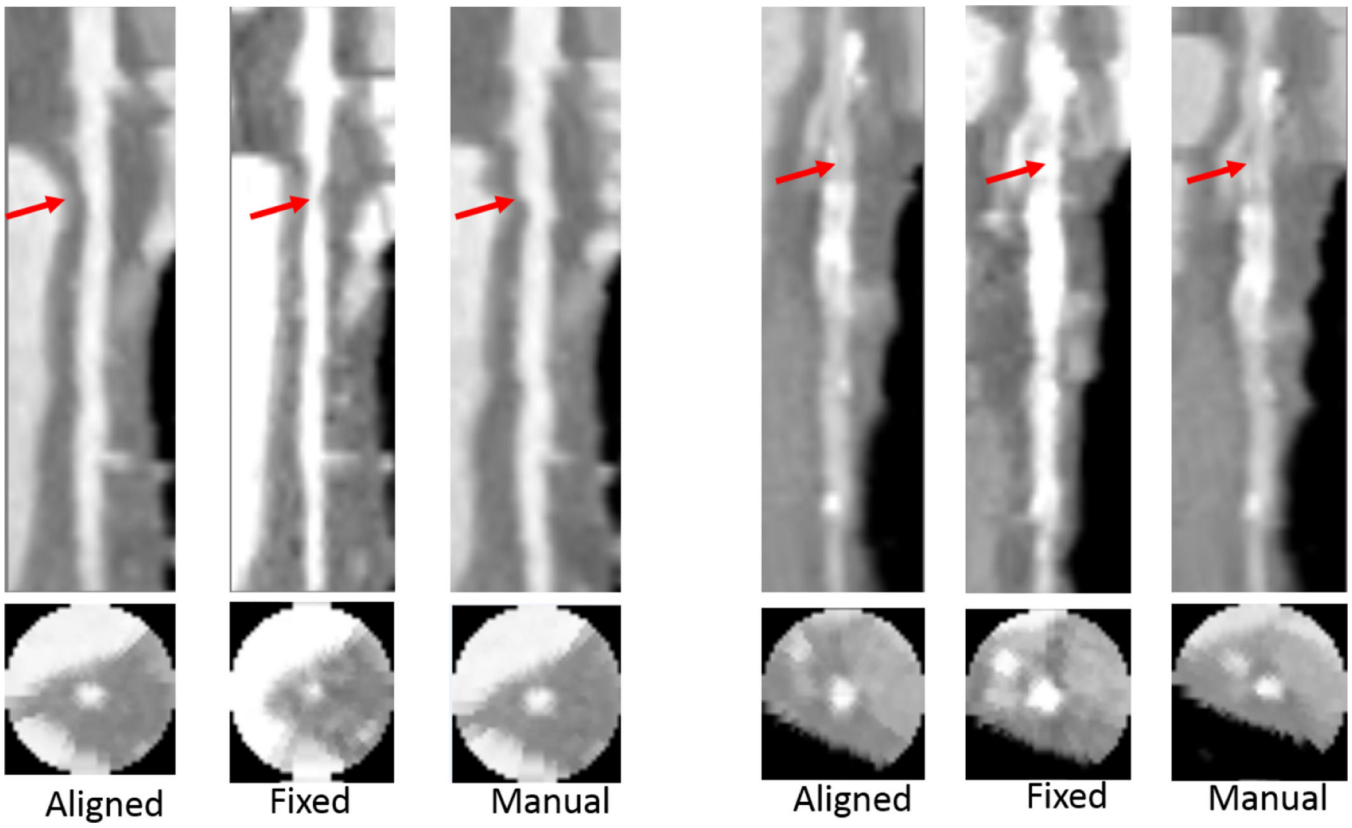

Fig. 5.
Cases of stenosis and calcification.

TABLE I

Parameters used in our algorithm.

Parameter(s)	Value
$\delta l, \delta\theta$	**1 mm,10°**
K	**10**
w_{img}, w_{geo}	**0.7,0.3**
s_{img}	**0.7**
Θ_{max}	**10°**
r_{min}, r_{max}	**0.8, 1.2**
R, δR	**10 mm, 0.5 mm**

TABLE II

Average distance error and standard deviation.

Artery Number	E_i (mm)	E_{g+i} (mm)
LAD_1	2.00 ± 0.90	1.89 ± 0.68
LCX_1	1.48 ± 1.05	1.25 ± 0.66
RCA_1	1.55 ± 0.87	1.33 ± 0.89
LAD_2	1.96 ± 1.45	1.39 ± 0.59
LCX_2	2.59 ± 1.99	1.50 ± 0.98
RCA_2	6.25 ± 6.04	2.12 ± 1.25
LAD_3	2.53 ± 1.60	2.08 ± 1.44
LCX_3	2.14 ± 2.69	2.03 ± 1.57
RCA_3	1.66 ± 1.13	1.14 ± 0.51
LAD_4	1.70 ± 1.08	1.35 ± 0.68
LCX_4	1.38 ± 0.63	1.19 ± 0.60
RCA_4	2.92 ± 2.05	1.75 ± 0.82
LAD_5	2.11 ± 1.58	1.28 ± 0.80
LCX_5	3.37 ± 2.90	1.49 ± 0.81
RCA_5	2.45 ± 1.54	2.19 ± 1.19
Average	2.40 ± 2.50	1.60 ± 1.00